INTERNATIONAL JOURNAL OF INTEGRATED ENGINEERING
ISSN: 2229-838X e-ISSN: 2600-7916

IJIE

Vol. 17 No. 8 (YEAR) 257-271
https://publisher.uthm.edu.my/ojs/index.php/ijie

Electrochemical Optimizing of SSC-SDCC Cathodes for LT-SOFCs: Synergistic Control of Composition, Phase Structure, Morphology, and Thermal Properties

Sufizar Ahmad[1]*, Umira Asyikin Yusop[1], Siti Fairus Mohammad[1], Hamimah Abd Rahman[1], Dedikarni Panuh[2], Joko Sedyono[3]

[1] *Faculty of Mechanical and Manufacturing, Universiti Tun Hussein Onn Malaysia, Parit Raja, Batu Pahat, 86400, MALAYSIA*
[2] *Department of Mechanical Engineering, Faculty of Engineering, Univesitas Islam Riau, INDONESIA*
[3] *Faculty of Engineering, Universitas Muhammadiyah Surakarta, INDONESIA*

*Corresponding Author: sufizar@uthm.edu.my
DOI: https://doi.org/10.30880/ijie.2025.17.08.022

Article Info

Received: 14 September 2025
Accepted: 2 December 2025
Available online: 31 December 2025

Keywords

ASR, composite cathode, HEBM, LT-SOFC, SSC-SDCC, TEC

Abstract

The growing global demand for alternative energy sources has driven the development of solid oxide fuel cells (SOFCs), which offer efficient and eco-friendly energy conversion. However, conventional SOFCs high operating temperatures accelerate material degradation, necessitating the exploration of low-temperature SOFC (LT-SOFC) materials. This study investigates samarium strontium cobalt-samarium doped ceria carbonate (SSC-SDCC) composite cathodes with varying weight ratios (50:50, 60:40, and 70:30, denoted as SSCB55, SSCB64, and SSCB73) mixed *via* high-energy ball milling (HEBM). The powders were calcined at 750°C, pelletised using the uniaxial pressing method, and sintered at 600°C. X-ray diffraction (XRD) analysis confirmed the formation of the $SrCO_3$ secondary phase, despite this phase formation, the cathode exhibited enhanced electrochemical performance with reduced ASR values. The energy dispersive spectroscopy (EDS) mapping demonstrated uniform elemental distribution across all samples, ensuring compositional homogeneity. The field emission scanning electron microscopy (FESEM) revealed microstructural evolution, including increased agglomeration after calcination process. Porosity measurement (31-44%) aligned with optimal cathode material requirements, facilitating efficient gas diffusion and electrochemical reactions. Thermal expansion coefficient (TEC) analysis indicated that only SSCB55 exhibited acceptable compatibility with the SDCC electrolyte, whereas SSCB64 and SSCB73 exceeded the recommended thresholds, risking mechanical failure during thermal cycling. Electrochemical impedance spectroscopy (EIS) further revealed that the SSCB55 cathode achieved low area specific resistance (ASR) by 5.06 Ωcm^2 at 600°C, indicating superior oxygen reduction reaction (ORR) kinetics and highlighting its potential for LT-SOFC applications. These findings suggest that optimised SSC-SDCC composites, particularly SSCB55, are promising candidates for high-performance LT-SOFC cathodes.

1. Introduction

Globally, the transition to clean energy technologies has become imperative as nations strive to meet climate commitments under the Paris Agreement, with particular emphasis on reducing carbon (CO_2) emissions from fossil fuel dependence [1]. In Malaysia, where energy production accounted for approximately 45% of total CO_2 emissions in 2022 [2], the need for sustainable alternatives is critical to align with the nation's pledge to achieve carbon neutrality by 2050. To address this challenge, Malaysia is exploring various renewable energy sources [3], including:

- Solar energy: Leveraging its tropical climate for photovoltaic systems.
- Hydropower: Expanding capacity through both large-scale and micro hydro projects.
- Biomass: Utilising agricultural waste for bioenergy production.
- Wind energy: Developing offshore wind potential in strategic locations.
- Hydrogen and fuel cell technologies: Emerging as a key solution for clean power generation.

Among these alternatives, fuel cell technology, particularly solid oxide fuel cells (SOFC), has gained significant attention due to its high efficiency (up to 60-85% in cogeneration systems) and low emissions profile [4]. Unlike intermittent renewable sources, like solar and wind power, which are dependent on weather conditions, SOFCs provide stable baseload power while emitting only water vapour as a byproduct when using hydrogen fuel [5]. This technology is particularly promising for Malaysia's energy transition, as it can be integrated with existing infrastructure and scaled for both urban and industrial applications. However, the widespread adoption of conventional SOFC technology has been hindered by its requirement for extremely high operating temperatures (800-1000°C), which leads to rapid material degradation and increased processing costs [6]. This challenge is particularly acute in Malaysia's tropical climate, where temperature and humidity fluctuations further stress energy systems.

Recognising these limitations, the global scientific community has turned its attention to developing low-temperature SOFCs (LT-SOFCs) capable of operating below 700°C while maintaining performance efficiency [7]. This shift has created new opportunities for Malaysia to leapfrog into next-generation energy technology by focusing on innovative cathode materials that combine thermal stability with excellent electrochemical performance at reduced temperatures. The development of advanced composites represents a crucial step in this direction, offering a pathway to make SOFC technology both environmentally sustainable and economically viable for Malaysia's unique energy landscape [8].

Perovskite-structured materials have emerged as highly promising cathode candidates for SOFCs, with $Sm_{0.5}Sr_{0.5}CoO_{3-\delta}$ (SSC) demonstrating exceptional electrochemical performance due to its high mixed ionic-electronic conductivity (MIEC) and superior oxygen reduction reaction (ORR) activity at intermediate temperatures [9]. The SSC perovskite's remarkable catalytic properties stem from its optimal oxygen vacancy concentration and stable cobaltite framework, facilitating rapid oxygen ion transport while maintaining structural integrity during operation [10]. Similarly, samarium-doped ceria carbonate (SDCC) composite has gained attention for its enhanced ionic conductivity and improved thermal compatibility with common electrolytes, achieved through the synergistic effect of samarium doping and carbonate phase incorporation [11]. The SDCC material system offers unique advantages, including extended triple-phase boundaries (TPB) and reduced interfacial resistance, making it particularly suitable for LT-SOFC applications [12].

Moreover, when combined in composite cathodes, these materials create a functionally graded system where SSC provides excellent electronic conductivity and electrocatalytic activity [13]. At the same time, SDCC ensures superior ionic transport and thermal expansion matching, addressing the critical challenges of conventional single-phase cathodes [14]. Although SSC and SDCC have been both demonstrated promising properties individually, the synergistic effects of SSC-SDCC composites on structural and thermal properties for LT-SOFCs below 600°C remain largely unexplored.

This study systematically investigates the optimisation of SSC-SDCC composite cathodes for LT-SOFCs through a comprehensive evaluation of compositional ratios. The research employs a multifaceted characterisation approach to elucidate the relationship between processing parameters and material properties, focusing on the critical role of stable chemical structure in maintaining phase purity and preventing detrimental secondary phase formation, while controlled particle size ensures optimal microstructural homogeneity and active surface area for ORR. Meanwhile, the tailored porosity influences gas diffusion kinetics and TPB density (where ionic/electronic conductors and gas phase intersect), directly impacting electrochemical performance [15].

Furthermore, the thermal stability of the composites is assessed to identify suitable processing conditions. A key focus lies in achieving thermal compatibility between the cathode and electrolyte layers, as mismatched thermal expansion coefficients (TEC) can lead to mechanical failure during cell operation. The TEC mismatch problem becomes particularly pronounced in SOFC systems due to the repeated thermal cycling between room temperature and operating temperature. When the cathode (typically with higher TEC values in the range of 12-

Int. Journal of Integrated Engineering Vol. 17 No. 8 (2025) p. 257-271

20 x 10^{-6} K^{-1}) and electrolyte (commonly 10-12 x 10^{-6} K^{-1} for SDCC) expand at different rates, the resulting stress accumulation can create microcracks that degrade the ionic pathway, increase interfacial resistance at critical boundaries, and ultimately shorten the operational lifespan of the cell [16]. This thermal stress degradation can be mitigated through, compositional tuning of the cathode to better match SDCC's TEC or microstructural engineering to create stress relieving pore networks while maintaining ionic percolation pathways.

The findings from this investigation are expected to provide fundamental insights into the design principles of advanced composite cathode materials, ultimately contributing to the realisation of more efficient and durable LT-SOFC systems operating in the 400-600°C range. By elucidating the synergistic effects through compositional tuning and calcination temperature, this work provides a scientific framework for optimising ionic-electronic conductivity, thermal expansion compatibility, and microstructural stability in composite cathode materials. The acquired dataset will serve as a valuable reference for future material optimisation efforts targeting reduced-temperature SOFC operation without compromising cell stability and performance.

2. Materials and Methods

The $Sm_{0.5}Sr_{0.5}CoO_{3-\delta}$-$Sm_{0.2}Ce_{0.5}O_{1.9}$ carbonate (SSC-SDCC) composite cathode powders were prepared using three distinct ratios (50:50, 60:40, and 70:30, designated as SSCB55, SSCB64, and SSCB73). Prior to mixing, the SDCC electrolyte composition was determined to consist of 80 wt.% samarium-doped ceria (SDC) (Kceracell, Korea) and 20 wt.% binary carbonates (Li_2CO_3: Na_2CO_3) (Sigma Aldrich, USA), which was thoroughly mixed *via* wet ball milling for 24 hours at 150 rpm, followed by calcination at 680°C for 1 hour. The SSC commercial powder (Kceracell, Korea) and SDCC composite were then mixed using high-energy ball milling (HEBM) (550 rpm within 2 hours) to ensure homogeneous mixing and nanoscale refinement in the making of SSC-SDCC composite cathode powder. The resulting powders underwent calcination at 750°C to optimise crystallinity and phase stability. Moreover, for material characterisation, composite cathode pellets and symmetrical cells were fabricated *via* uniaxial pressing to evaluate porosity and electrochemical properties. Symmetrical cells were prepared in an electrolyte-supported configuration with a cathode-electrolyte-cathode design. Both the pellets and symmetrical cells were sintered at 600°C for 1 hour to ensure structural integrity and optimal performance.

Subsequently, the characterisation of SSC-SDCC composite cathode powder was then examined for their phase identification conducted *via* X-ray diffraction (XRD, D8 Advanced Bruker, Germany) to assess crystallinity and phase purity. The physical properties, including elemental distribution, powder morphology, porosity density and was characterised using advanced analytical techniques. Field emission scanning electron microscopy (FESEM, JEOL JSM-7600F, Japan), coupled with energy dispersive spectroscopy (EDS), was employed to examine the elemental composition and microstructure. Porosity and density measurements were performed using a precision density kit (Density Kit XP, Mettler Toledo, USA), the reported values are the average of five independent measurement, with an estimated error of ±2%.

Additionally, the thermal expansion coefficient (TEC) was measured *via* a dilatometer (L75H, Linseis, Germany) to assess thermal compatibility between the composite components. Each TEC value reported represents the mean of three consecutive heating/cooling cycles, and the standard deviation was within ±1.0 x $10^{-6}K^{-1}$. Electrochemical performance was evaluated (400-600°C) through electrochemical impedance spectroscopy (EIS) using an Autolab PGSTAT302N potentiostat coupled with an impedance analyser (Autolab 302, Eco Chemie, Netherlands) to determine the ionic and electronic conductivity of the composite cathode. The area-specific resistance (ASR) values were obtained from the EIS data, and the measurements were repeated three times at each operating temperature to ensure the consistency of the measurements. Fig. 1 below illustrates the flow chart of the experiments.

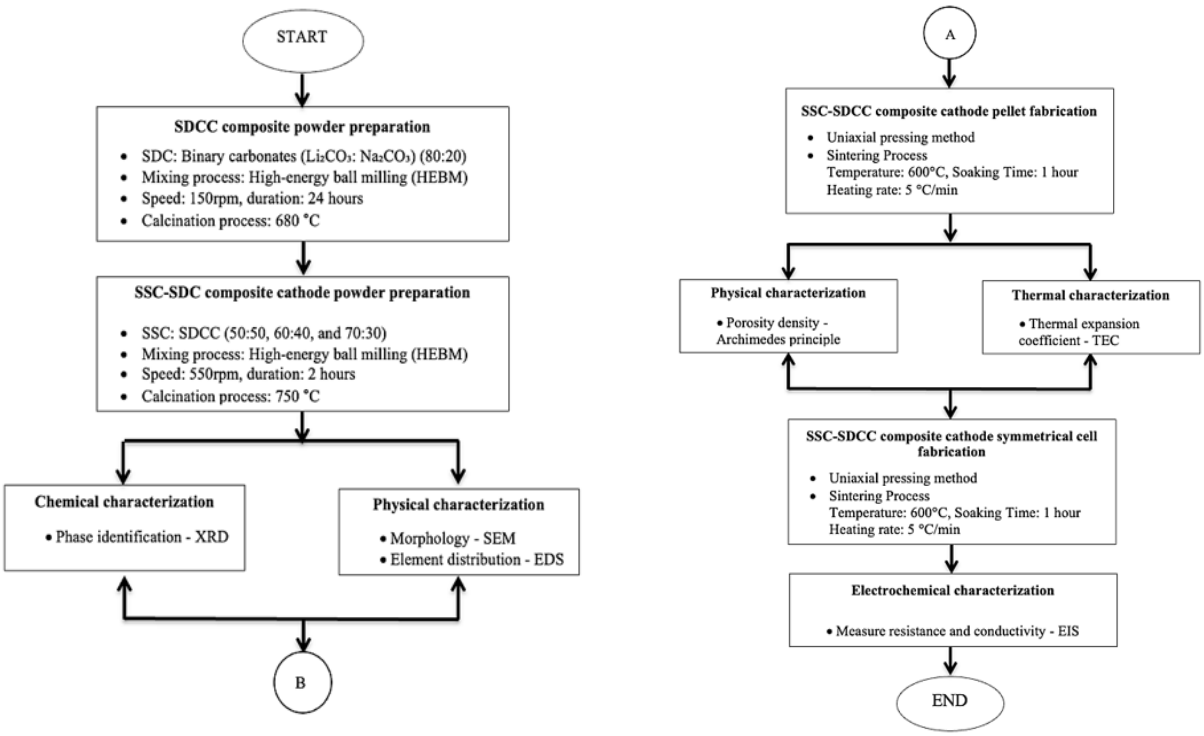

Fig. 1 *A schematic flow chart illustrating the experimental procedure*

3. Results and Discussion

This section presents the experimental findings and their implications for the SSC-SDCC composite cathodes in LT-SOFC applications. Through systematic characterization (XRD, EDS, FESEM, porosity density, TEC and EIS), the relationship between composition, microstructure, and performance can be elucidated. Key focus area includes the role of $SrCO_3$ secondary phases in conductivity enhancement, thermal expansion compatibility between cathode and electrolyte and the electrochemical optimization of composite cathodes. These results provide actionable insights for material design and operational stability in LT-SOFCs systems.

3.1 Phase Structure Identification

The XRD diffractograms of pure SSC, pure SDC carbonate (SDCC), and the as-prepared SSCB55, SSCB64, and SSCB73 composite cathodes are presented in Fig. 2. The XRD spectra of SSC and SDCC powders exhibited characteristic peaks corresponding to their respective reference phases: SSC displayed an orthorhombic perovskite structure (JCPDS No. 53-0112), while SDCC showed a face-centred cubic fluorite structure (JCPDS No. 75-0158). The XRD patterns did not reveal the presence of carbonate phases, as the carbonate layer uniformly coated the SDC particle and remained in an amorphous state, leaving the fluorite structure of SDC unaltered [17]. Notably, even after the HEBM process, the amorphous nature of the carbonate species was preserved without disruptions. Furthermore, as the SDCC content increased across the composite series, a systematic reduction in SSC peak intensity was observed alongside a corresponding enhancement in SDCC peak intensity, confirming the progressive phase dominance of SDCC in the composite structure. These results demonstrate that the HEBM method, with proper selection of milling parameters, successfully produced well-structured SSC-SDCC composite powders while maintaining the integrity of both crystalline and amorphous phases. This is effective for compositional modulation achieved through the controlled variation of SSC-SDCC ratios while maintaining structural integrity.

Notably, the composite cathodes retained the distinct phases of both SSC and SDCC, with no observable secondary phases, confirming the successful formation of the intended perovskite-fluorite composite system without chemical interaction between the constituent materials. The presence of well-defined peaks in all samples indicates high crystallinity and phase purity, essential for optimal electrochemical performance [18]. Considering these findings, the HEBM method even at a high milling speed of 550 rpm are proved effectively produce well dispersed SSC-SDCC composite cathode powders with homogeneous phase distribution and improved interfacial contact.

Int. Journal of Integrated Engineering Vol. 17 No. 8 (2025) p. 257-271

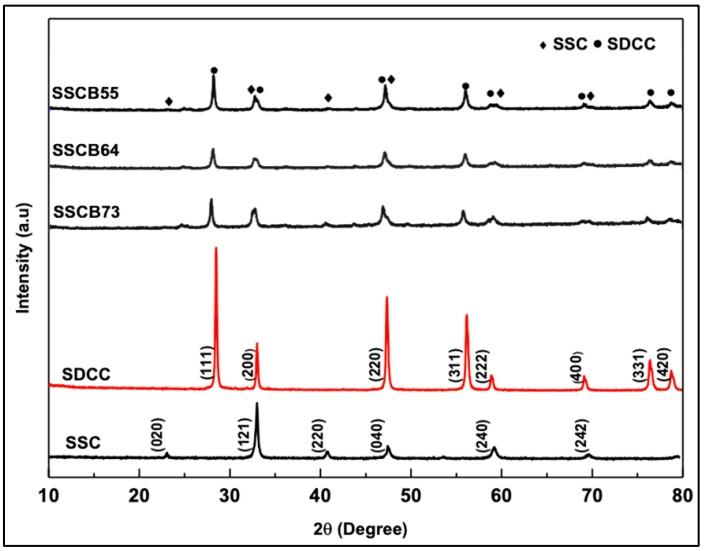

Fig. 2 *X-ray diffraction spectra (Cu Kα radiation, 2θ = 10-80 ° with a step size of 0.02 °) for commercial SSC, SDCC powder, and the as-prepared SSCB55, SSCB64 and SSCB73 composite cathode powders*

Fig. 3 presents the XRD diffractograms of calcined SSC-SDCC composite cathode at 750°C, alongside reference patterns of commercial SSC and SDCC composite electrolyte. Notably, the calcined composite (SSCB55, SSCB64, and SSCB73) exhibited distinct secondary peaks corresponding to strontium carbonate ($SrCO_3$), which emerged between 2θ = 25-50° across all compositions. Based on the figure, the secondary phase intensities show varied composition dependently, which SSCB73 showed the weakest $SrCO_3$ peaks, followed by SSCB64 and SSCB55 demonstrating the most pronounced formation. This phenomenon likely originated from reactions between strontium precursors and residual carbon dioxide or sodium carbonate (Li_2CO_3/Na_2CO_3) during preparation process [19].

The identification of $SrCO_3$ secondary phases is consistent with documented behaviour in perovskite oxide systems, where its controlled presence is common occurrence in such mixing and syntheses process [20]. While the primary perovskite structure remains dominant, the presence of $SrCO_3$ warrants consideration of its potential role. It could potentially form a passive, insulating phase that might block active sites. Conversely, it is also plausible that it modifies ionic pathways at the grain boundaries, influencing oxygen surface exchange and transport. Crucially, subsequent EIS and polarization measurements revealed that the $SrCO_3$ formation did not adversely impact cathode performance metrics such as ASR or ORR activity. This suggests that its influence is either minimal or its effects are counterbalanced within the composite. Further investigation to elucidate potential synergistic effects on cathode performance, particularly regarding stability and ionic transport.

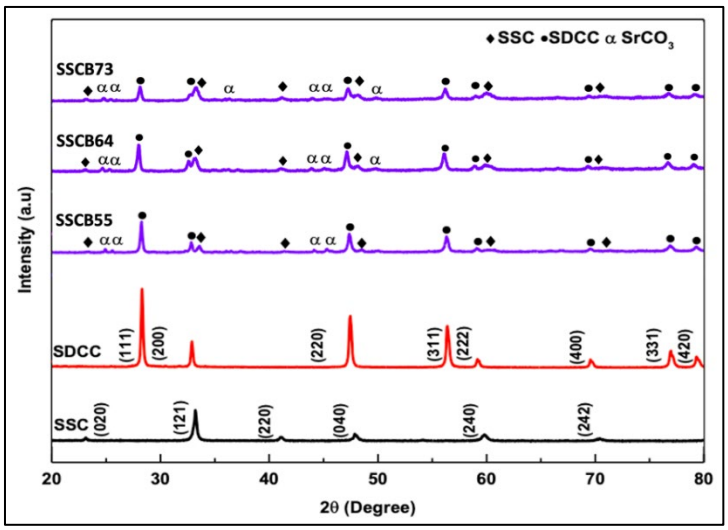

Fig. 3 *XRD diffractogram (Cu Kα radiation, 2θ = 10-80 ° with a step size of 0.02 °) of commercial SSC, SDCC, and SSCB55, SSCB64, SSCB73 composite cathode powders after calcination process*

3.2 Elemental Distribution Analysis

The compositional homogeneity of SSC-SDCC composite cathode powders was further evaluated by using FESEM coupled with EDS analysis following HEBM processing. Figs. 4 and 5 presents the elemental mapping for both as-prepared and calcined SSC-SDCC composites. The elemental mapping of as-prepared SSCB55 (Fig. 4(a)) revealed a uniform distribution of all major constituent elements (Na [4a(b)], Co [4a(c)], Sr [4a(d)], Ce [4a(e)], and Sm [4a(f)]), confirming effective homogenization through HEBM. Notably, lithium (Li) was not detected in the EDS spectrum, due to its low atomic mass limitations [21]. Quantitatively, the EDS analysis demonstrated composition dependent trends. The SSCB55 sample exhibited the highest Na content (Fig. 4(a)), while SSCB73 showed elevated Sr concentrations (Fig. 4(c)), as detailed in table attached at every EDS graph below. This correlation aligns perfectly with the designed carbonate and SSC ratios in each composite. The observed elemental uniformity is critical for optimizing ORR kinetics and electrochemical performance, as homogeneous elemental distribution enhances active site accessibility and charge transfer efficiency [22]. Importantly, the HEBM process parameters successfully achieved the desired nanoscale mixing, with no elemental segregation in any composite formulation. These results, supported by both visual mapping and quantitative data, validate the efficacy of HEBM for preparing high-quality composite cathodes with controlled stoichiometry and element distribution.

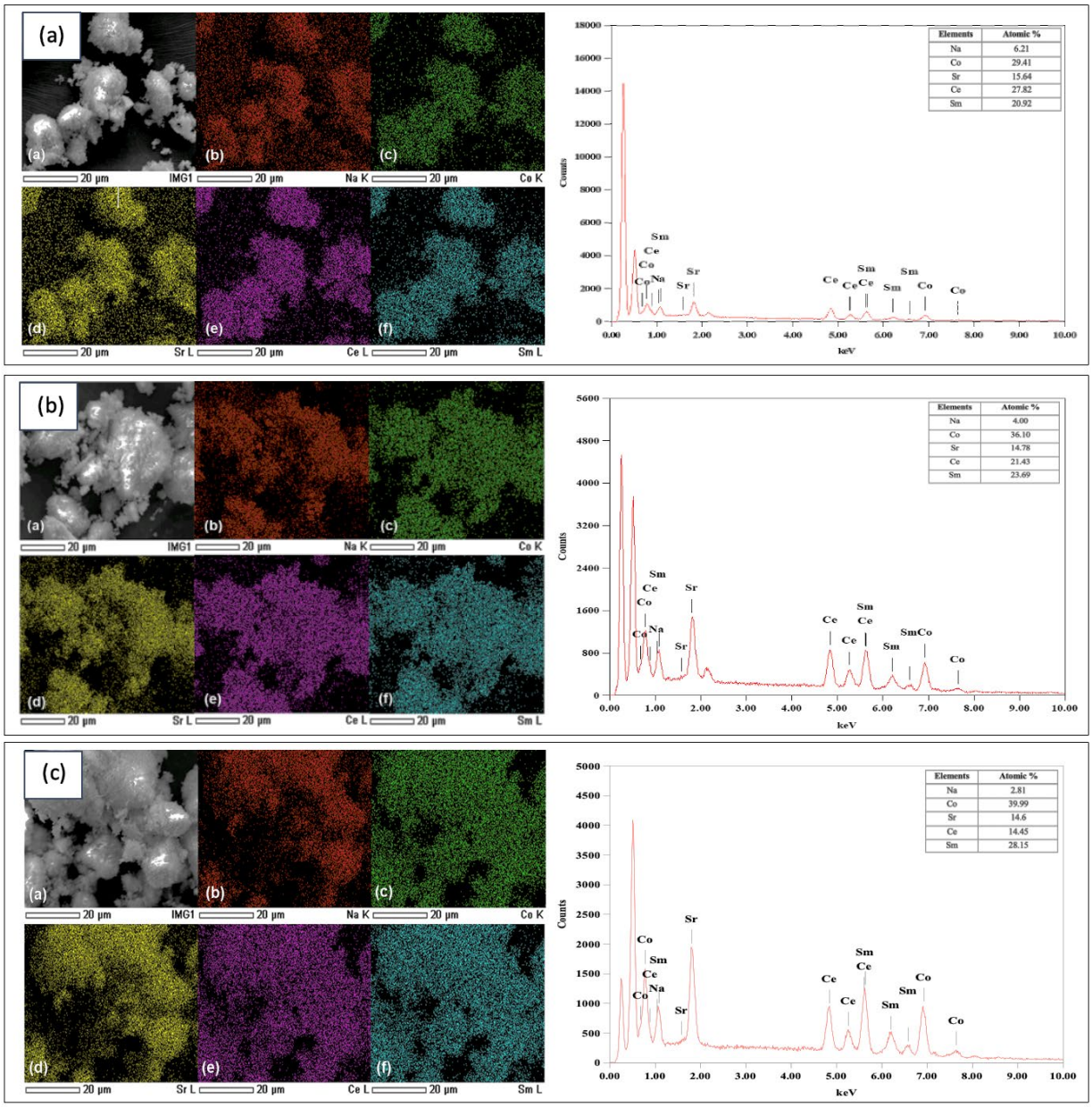

Fig. 4 *Elemental distribution analysis of as-prepared SSC-SDCC composite cathode (a) SSCB55; (b) SSCB64; (c) SSCB73*

Int. Journal of Integrated Engineering Vol. 17 No. 8 (2025) p. 257-271

The FESEM-EDS analysis in Fig. 5 confirms the uniform distribution of all major elemental constituents within the calcined SSC-SDCC composite powders. This nanoscale compositional homogeneity directly translates to electrical homogeneity, ensuring a continues network for ion and electron transport. Such a uniform environment is crucial for ORR activity, as it maximizes the density and accessibility of triple-phase boundaries (TPBs), which serve as an active site where oxygen, electrons, and ions converge. A homogenous distribution prevents the formation of localized inactive regions with poor conductivity, thereby facilitating efficient oxygen surface exchange and bulk diffusion. The preservation of elemental uniformity after calcination suggests that the HEBM derived precursor powders possess inherent thermal stability, enabling the reproducible fabrication of composite cathodes with optimized microstructural for enhanced electrochemical performance [23]. The plotted graph quantifies the atomic percentages of all major constituent elements in the SSC-SDCC composite cathode powders.

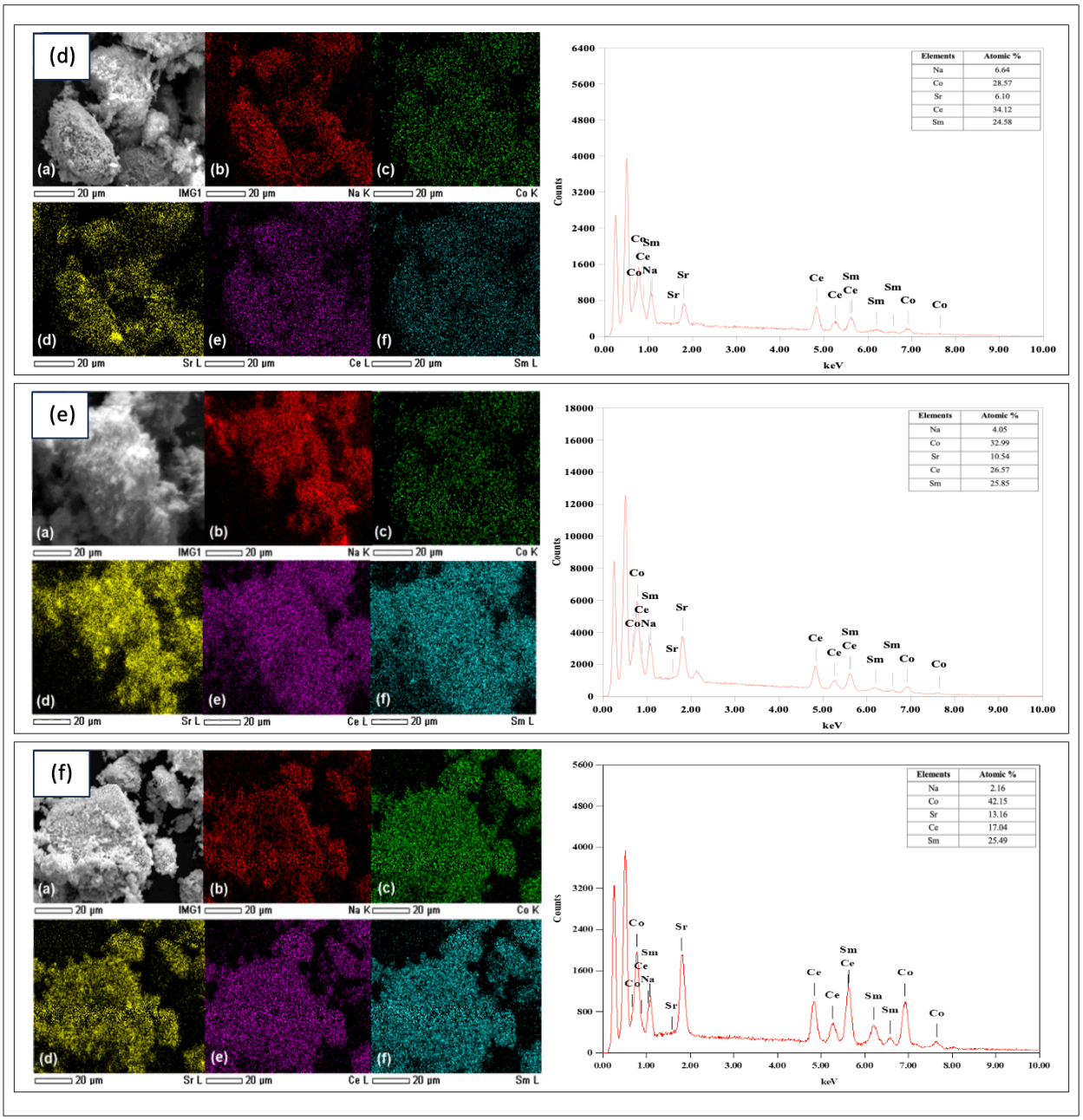

Fig. 5 *Elemental distribution analysis of calcined SSC-SDCC composite cathode (a) SSCB55; (b) SSCB64; (c) SSCB73*

3.3 Microstructural and Morphological Analysis

All FESEM micrographs presented in this study were obtained after HEBM processing, which mechanically breakages particles into fine, well-distributed powders through intense impact and shear forces [24]. As demonstrated by Lun Feng et al. [24], HEBM effectively refines particle phases and enhances interfacial contact between mixed powders, thereby increasing the specific surface area of SSC-based composite cathodes within a remarkably short processing time (2 hours in this study). Fig. 6 compares the morphological evolution across processing stages, showing raw SSC, as-prepared SDCC, and both as-milled and calcined SSC-SDCC powders. While HEBM initially produces nanoscale particles (20-50 nm), subsequent calcination at 750°C induces soft agglomeration due to weak interparticle bonding from surface energy minimization. Crucially, the aggregates formed (particularly in SSCB73 compared to SSCB64 and SSCB55) remained porous and were readily dispersed, preserving the essential nanoscale features and high active surface area necessary for efficient gas diffusion and change transfer. This behaviour aligns with calcination theory, where elevated temperatures promote bonding while aiming to maintain the intrinsic homogeneity achieved by HEBM [25], [26]. The composition dependent cohesion strength, with SSCB73 forming rougher aggregates, suggests a link between stoichiometry, sintering behaviour, and the resulting electroactive microstructure.

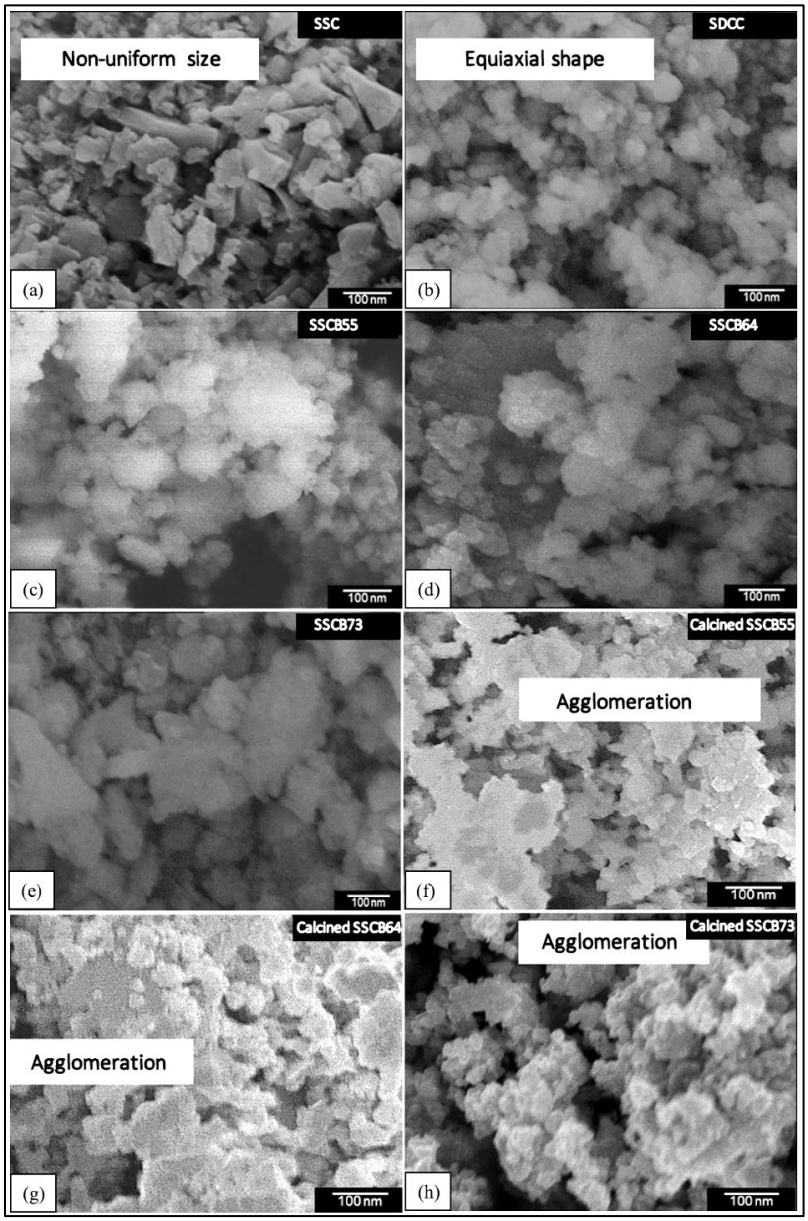

Fig. 6 *FESEM morphology of (a) Commercial SSC; (b) SDCC electrolyte, and as-prepared SSC-SDCC composite cathode; (c) SSCB55; (d) SSCB64; (e) SSCB73 also calcined SSC-SDCC composite powder; (f) SSCB55; (g) SSCB64; (h) SSCB73*

Int. Journal of Integrated Engineering Vol. 17 No. 8 (2025) p. 257-271

3.4 Apparent Porosity and Density

This section presents a systematic investigation of the physical properties of SSC-SDCC composite cathode pellets, focusing on the effects of compositional on apparent porosity and bulk density. The quantitative results, tabulated in Table 1 and graphically represented in Fig. 7, reveal distinct trends in these microstructural characteristics. As the increasing SSC content in the SSC-SDCC composite cathode composition, the apparent porosity increased from SSCB55 to SSCB64 and decrease to SSCB73, while the bulk density steadily decreased from SSCB55 to SSCB73. The porosity reduction mechanism operates through two complementary pathways; (i) particle coarsening during calcination, which decreases surface area and promotes densification, and (ii) controlled agglomeration that enhances particle packing efficiency [27].

In addition, with pellet pressing it can effectively eliminate soft agglomerates that formed during calcination, but on hard agglomerates persist as evidenced by FESEM analysis at Section 3.3. These residual agglomerates contribute to the porosity profile, with SSCB55 and SSCB64 showing more pronounced agglomeration compared to SSCB73. The findings by Liu et al. [28] further support this interpretation, confirming that mechanical pressing only partially mitigates the porosity introduced by calcination-induced agglomeration. The observed porosity density relationship significantly impacts cathode performance, as it directly influences both gas diffusion pathways and electrochemical active sites [29].

Besides, the formation of $SrCO_3$ secondary phases during calcination exhibits an inverse relationship with porosity reduction in SSC-SDCC composite cathodes. As demonstrated in Section 3.1, calcined SSCB55 and SSCB64 compositions showed minimal $SrCO_3$ formation, which correlates with their lower porosity values. This observation aligns with established materials sciences principles where secondary phases typically inhibit densification by creating microstructural defects and pore stabilization sites [30]. Extensive studies in SOFC research have established that optimal ionic conductivity in cathode materials is achieved when the porosity ranges between 20-40%, with peak performances typically observed at approximately 30% porosity [31]. While the calcined SSC-SDCC composite cathode (SSCB55, SSCB64, and SSCN73) exhibited slightly fluctuated porosity values (35.43-38.57%), these measurements remain within a functionally relevant range for cathode operation. The observed porosity characteristics, coupled with complementary density measurements, confirm that all three compositions maintain suitable microstructural properties for practical application.

Table 1 *The average of porosity and density values of calcined SSC-SDCC composite cathode pellets*

SSC-SDCC composite cathode	Porosity (%)	Density (gcm^{-1})
SSCB55	35.43 ± 0.22	5.26 ± 0.02
SSCB64	38.57 ± 1.82	5.27 ± 0.28
SSCB73	37.69 ± 0.84	5.30 ± 0.15

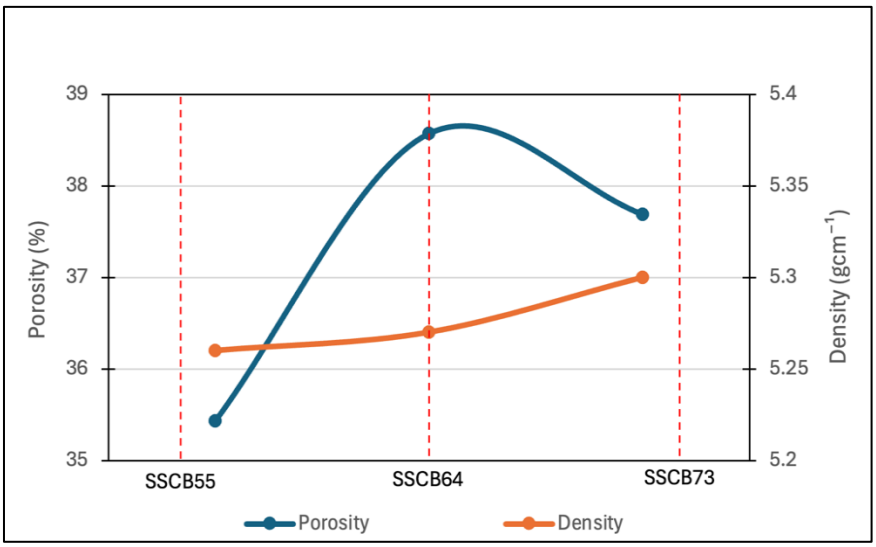

Fig. 7 *The average of porosity and density value for SSC-SDCC composite cathode pellets with varying weight ratio*

3.5 Thermal Compatibility of Cell Components

Thermodynamic compatibility, particularly TEC matching between cathode and electrolyte, represents a critical design criterion for SOFCs. Cobalt-rich cathodes such as SSC presents a significant challenge in this regard, as typically exhibit high TEC values (12-20 x 10^{-6} K^{-1}), compared to the lower TEC of common electrolyte (10-12 x 10^{-6} K^{-1}) [32]. This mismatch induces substantial thermal stresses during heating cycles, leading to detrimental interfacial delamination and microcrack formation at the cathode/electrolyte interface [33]. As quantified in Table 2 and graph trend in Fig. 8, the developed SSC-SDCC composite cathodes demonstrate improved thermal expansion behaviour through strategic compositional tuning, effectively mitigating these stress related degradation mechanisms while maintaining electrochemical performance.

Table 2 *The thermal expansion behaviours of SSC-SDCC composite cathodes at temperature 30-600 ℃*

Composite pellets	TEC value (x 10^{-6} K^{-1})	TEC mismatch (%)
SDCC	11.1 ± 0.3	-
SSCB55	12.0 ± 0.4	8.1
SSCB64	16.0 ± 0.1	44.1
SSCB73	17.0 ± 0.9	53.2

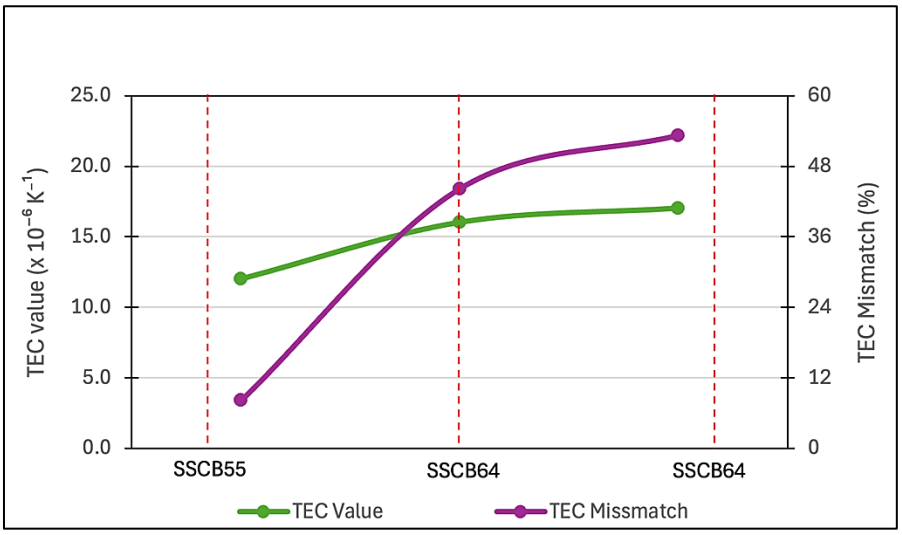

Fig. 8 *The TEC value and mismatch percentage of SSC-SDCC composite cathode pellets with modifying weight ratio*

Thermal expansion compatibility analysis reveals significant improvements in the SSC-SDCC composite cathode systems, as detailed in Table 2 and Fig. 8. Based on the table, SDCC electrolyte have an average TEC value of 11.1 x 10^{-6} K^{-1} and conventional SSC cathodes exhibit substantially higher values, the composite effectively addresses this mismatch. Systematic incorporation of SDCC electrolyte progressively reduce the composite TEC, with SSB55 demonstrating optimal thermal compatibility (12.0 x 10^{-6} K^{-1}), closely matching the SDCC electrolyte across all composite pellets. This represents a 30-40% reduction compared to standard SSC-based cathodes, achieving values within the ideal operational range (10-13 x 10^{-6} K^{-1}) for SOFC components [34]. These findings demonstrate that electrolyte content effectively tunes thermal expansion in SSC-SDCC cathodes, resolving cobaltite limitations while maintaining their advantageous electrochemical properties.

Moreover, the increasing of TEC values with higher SSC content are shown directly correlated with the agglomeration phenomena observed in FESEM analysis in Section 3.3. This behaviour aligns with established nanocomposite principles [35], where homogeneous dispersion of fine particles as in SSCB55, yields superior thermo-mechanical properties and lower TEC values, while particle agglomeration prominent in SSCB64 and SSCB73, detrimentally increase thermal expansion. Quantitative analysis shows the SSCB55-SDCC system maintains exceptional thermal compatibility, with only 8.1% TEC mismatch and its well within the 20% threshold for thermodynamic compatibility [36]. In contrast, SSCB64 and SSCB73 exceed this limit by 44.1% and 53.2% respectively.

In a stress-strain perspective, this significant TEC mismatch generates substantial interfacial shear stresses during thermal cycling. Under repeated cyclic loading, this accumulated strain energy promotes crack initiation and propagation, ultimately resulting in layer delamination. These interfacial thermal stresses compromise mechanical stability during thermal cycling [37]. These results conclusively identify SSCB55 as the optimal

composition, demonstrating superior TEC compatibility while maintaining electrochemical functionality which is key requirements for durable SOFC operation, and this compositional will be further investigated to validate its performance. The findings establish how microstructural control through compositional optimization can effectively mitigate one of the most challenging limitations in cobaltite cathode applications.

3.6 Electrochemical Performance

This section elaborates on the electrochemical impedance spectra of SSB55 composite cathode measured under open-circuit conditions in air across the temperature range of 450-600°C. Table 3 and Fig. 9 recorded the ASR value and trends of these findings that were fitted using equivalent circuit model $R_0/(R_1\text{-CPE})/(R_2\text{-CPE})/(R_3\text{-CPE})$. The plot in Fig. 9 includes magnified views of select curves to clarify subtle features at different frequency scales. On this study, the focus specifically on the ASR derived from the impedance data, as it directly reflects the cathode's electrochemical performance. The impedance spectra in Fig. 9 exhibit characteristic semi-circular arc above the real axis, followed by low-frequency tails, representing the electrochemical processes in the SSB55 composite cathode. ASR values demonstrate decreased dramatically from 53.93 Ωcm^2 at 450°C to 5.06 Ωcm^2 at 600°C. This reduction attributed to microstructural evolution and enhanced ionic conduction. The molten carbonate phase particularly enhances charge transfer by creating percolating ionic networks at SSCB55 interfaces, effectively expanding the active sites for ORR [20].

Table 3 *The ASR values of SSCB55 at operating temperature of 450-600 ℃*

Operating temperature (°C)	ASR values (Ωcm^2)
450	53.93
500	10.97
550	10.06
600	5.06

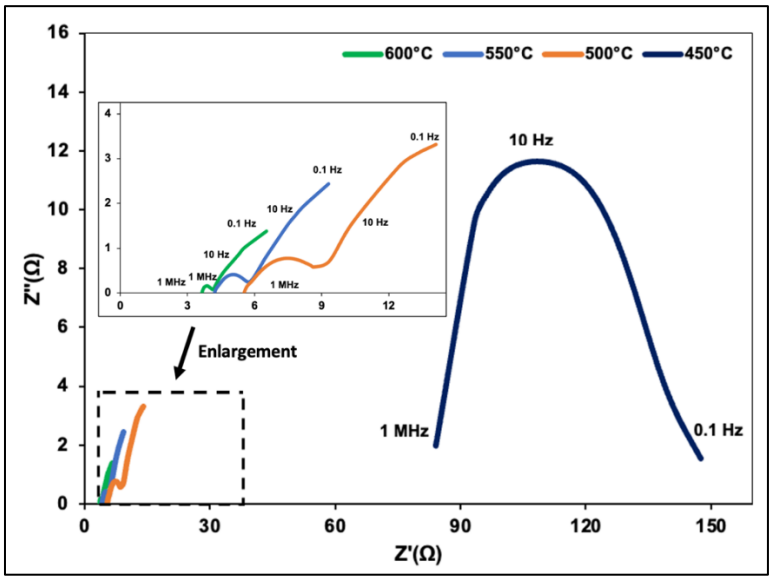

Fig. 9 *The Nyquist plot of SSCB5 operated at 450-600 ℃*

A distinct transition in electrochemical behaviour is observed when operating temperatures fall below the carbonate melting point (~450°C). In this regime, the impedance spectra exhibit enlarged semi-circular arcs disappearance of the low-frequent tail, indicative of compromised ionic transport [38]. As established in Section 3.1, the formation of $SrCO^3$ secondary phases in SSCB55 composites affected oxide ion (O^{2-}) transport at cathode-electrolyte interfaces. While the MIEC properties of SSC facilitate ORR across the entire cathode surface, $SrCO^3$ phases introduce unfavourable functions that elevate ASR. Besides, there have been a reliable suggestion that the existence of a small number of secondary phases from SSC cathode assisted in the better cell performance [39]. Strategic carbonate incorporation into the SDC electrolyte has proven effective by creating additional ionic conduction networks that compensate for SSC instability [40]. EIS analysis confirms that these composite cathodes achieve acceptable performance at lower temperatures, with an ASR of 5.06 Ωcm^2 at 600°C. A comparison with the prior work of Hui Deng et al. [41] underscores a key improvement with their SSC-GDC

cathode has an ASR range of 0.3-1.1 Ωcm^2 at operating temperature 630-780°C. In contrast, the SSC-SDCC cathode achieves in this study are comparable and even superior minimum ASR (5.06 Ωcm^2) at a much lower temperature of 600°C. This successful shift of high-performance operation to a lower thermal regime highlights the efficacy of the SDCC composite in enhancing oxygen ion kinetics and reducing interfacial resistance at reduced temperatures.

The microstructural optimization of SSCB55 cathodes demonstrates a clear correlation between porosity and electrochemical performance, with ideal ASR achieved at 35.43% porosity. This aligns with the established porosity range (20-40%) required for effective oxygen transport to active reaction sites while maintaining structural integrity [31]. In addition, the superior performance of SSCB55 is further attributed to its exceptional thermal compatibility with SDCC electrolyte, exhibiting only 8.1% TEC mismatch. This minimal discrepancy collectively contributing to its achieved ASR of 5.06 Ωcm^2 at 600°C. A reduction in ASR, which signifies lower polarization resistance, facilitates more efficient electrode kinetics and thereby lead to a higher overall cell performance.

4. Conclusions

This comprehensive study elucidates the critical structure property relationships in SSC-SDCC composite cathodes through systematic characterization of chemical compatibility, microstructure, physical properties, thermal behaviour, and electrochemical performance. Both SSC (orthorhombic) and SDCC (face-centred cubic) phases maintain their structural integrity after processing, with SrO^3 secondary phase formation. Among the investigated compositions, SSCB55 demonstrates optimal performance, exhibiting: (i) exceptional chemical compatibility with less formation of $SrCO_3$, (ii) ideal porosity with 35.43% for gas diffusion and TPB formation, and (iii) greater TEC mismatch with only 8.1% different to SDCC electrolyte (SSCB55 = 12.0 x 10^{-6} K^{-1} and SDCC = 11.1 x 10^{-6} K^{-1}), and (iv) superior electrochemical activity by low ASR value, 5.06 Ωcm^2 at 600°C. The enhanced electrocatalytic performance at elevated temperatures stems from synergistic effects between the SSC cathode and SDCC electrolyte, particularly through improved ionic conduction pathways. These findings collectively establish SSCB55 as a highly promising cathode material for LT-SOFCs, achieving an optimal balance between thermo-mechanical stability and electrochemical functionality through careful compositional optimization.

Acknowledgement

This research was supported by Universiti Tun Hussein Onn Malaysia (UTHM) through Tier 1 (Vot Q926).

Conflict of Interest

Authors declare that there is no conflict of interests regarding the publication of the paper.

Author Contribution

The authors confirm contribution to the paper as follows: ***study conception and design:*** *Sufizar Ahmad, Umira Asyikin Yusop, Siti Fairus Mohammad, Hamimah Abd Rahman, Dedikarni Patuh, Joko Sedyono;* ***data collection:*** *Sufizar Ahmad, Siti Fairus Mohammad, Hamimah Abd Rahman,* ***analysis and interpretation of results:*** *Umira Asyikin Yusop, Siti Fairus Mohammad;* ***draft manuscript preparation:*** *Sufizar Ahmad, Umira Asyikin Yusop, All authors reviewed the results and approved the final version of the manuscript.*

References

[1] Xuelin Tian, Chunjiang An & Zhikun Chen (2023) The role of clean energy in achieving decarbonization of electricity generation, transportation, and heating sectors by 2050: A meta-analysis review, *Renewable and Sustainable Energy Reviews*, *182,* 113404, https://doi.org/10.1016/j.rser.2023.113404

[2] IEA (2025, August). *Greenhouse Gas Emissions from Energy, IEA, Paris*. Licence: Terms of Use for Non-CC Material. https://www.iea.org/data-and-statistics/data-product/greenhouse-gas-emissions-from-energy

[3] Nik, N. N. A. (2024, October 18). National Climate Change Policy 2.0 (NCCP 2.0). Malaysia's Ministry of National Resources and Environmental Sustainability. Retrieved July 24, 2025, from https://www.nres.gov.my/msmy/pustakamedia/Penerbitan/National%20Policy%20on%20Climate%20Change%202.0.pdf

[4] Lina Hamid, Omer Elmutasim, Dattatray S. Dhawale, Sarbjit Giddey & Gary Paul (2024) Comparative electrochemical performance of solid oxide fuel cells: Hydrogen vs. ammonia fuels—A mini review, *Processes*, *13(4),* 1145, https://doi.org/10.3390/pr13041145

[5] Mariana Pimenta Alves, Waseem Gul, Carlos Alberto Cimini Junior & Sung Kyu Ha (2022) A review on industrial perspectives and challenges on material, manufacturing, design and development of compressed hydrogen storage tanks for the transportation sector, *Energies, 15(14)*, 5152, https://doi.org/10.3390/en15145152

[6] Kairat A Kuterbekov, Asset M Kabyshev, Kenzhebatyr Zh Bekmyrza, Marzhan M Kubenova, Gaukhar Kabdrakhimova, Iroda Abdullayeva & Abebe Temesgen Ayalew (2025) Advancements in electrolyte materials and hybrid integration for enhanced solid oxide fuel cell performance, *International Journal of Low-Carbon Technologies*, *20*, 353-367, https://doi.org/10.1093/ijlct/ctaf007

[7] Inkollu Sreedhar, Bhawana Agarwal, Priyanka Goyal, & Ankita Agarwal (2020) An overview of degradation in solid oxide fuel cells-potential clean power sources, *Journal of Solid-State Electrochemistry*, *24*, 1239-1270, https://doi.org/10.1007/s10008-020-04584-4

[8] Khaled M. A. Salim, Ruhanita Maelah, Hawa Hishamuddin, Amizawati Mohd Amir & Mohd Nizam Ab Rahman (2022) Two decades of life cycle sustainability assessment of solid oxide fuel cells (SOFCs): A review, *Sustainability*, *14(19)*, 12380, https://doi.org/10.3390/su141912380

[9] Rameez Ali, Khalid Aljohani, Sarfraz Ali, Shahzad Rasool, Atif Nazar, Tariq Bashir, Zhan Gao, Rizwan Raza & Muhammad Imran Asghar (2025) Insight of potentials for perovskite cathode materials for solid oxide fuel cell and semiconductor membrane fuel cells, *Ceramics International*, *51(19-B)*, 28477-28503, https://doi.org/10.1016/j.ceramint.2025.04.084

[10] Ahmed Badreldin, Aya E. Abusrafa & Ahmed Abdel-Wahab (2020) Oxygen-deficient perovskites for oxygen evolution reaction in alkaline media: A review, *Emergent Material*, *3*, 567-590, https://doi.org/10.1007/s42247-020-00123-z

[11] Burcu Aygun, Vedat Sariboga & Mehmet Ali Faruk Oksuzomer (2021) Effect of fuel choice on conductivity and morphological properties of samarium doped ceria electrolytes for IT-SOFC, *Turkish Journal of Chemistry*, *45(5)*, 1408-1421, https://doi.org/10.3906/kim-2104-56

[12] Jorgensen, Peter Stanley, Ebbehoj, Soren Lyng & Hauch Anne (2015) Triple phase boundary specific pathway analysis for quantitative characterization of solid oxide cell electrode microstructure, *Journal of Power Sources*, *279*, 686-693, https://doi.org/10.1016/j.jpowsour.2015.01.054

[13] Arim Seong, Donghwi Jeong, Minseo Kim, Sihyuk Choi & Guntae Kim (2022) Performance comparison of composite cathode: Mixed ionic and electronic conductor and triple ionic and electronic conductor with $BaZr_{0.1}Ce_{0.7}Y_{0.1}Yb_{0.1}O_{3-\delta}$ for highly efficient protonic ceramic fuel cells, *Journal of Power Sources*, *530*, 231241, https://doi.org/10.1016/j.jpowsour.2022.231241

[14] Maria Carmenza Diaz Lacharme, Andrea Bartoletti, Katia Monzillo, Riccardo Ceccato, Francesco Parrino, Emanuela Callone, Sandra Dire, Vincenzo Vaiano, Alessandra Sanson, Angela Gondolini & Alessandro Donazzi (2025) Sintering-driven optimization of multi-ionic SDC-Na_2CO_3 nanocomposite electrolytes for low-temperature solid oxide cell applications, *Fuel Processing Technology*, *276*, 108284, https://doi.org/10.1016/j.fuproc.2025.108284

[15] Davide Cademartori, Davide Clematis & Maria Paola Carpanese (2024) Microstructural and electrochemical properties of Ni-impregnated GDC10 and 8YSZ freeze tape cast scaffolds as fuel electrodes for solid oxide cells, *International Journal of Hydrogen Energy*, *50-C*, 1050-1063, https://doi.org/10.1016/j.ijhydene.2023.10.027

[16] Lin Zhuang (2021) Offsetting the thermal expansion mismatch: a new way to high-performance solid oxide fuel cell cathodes, *Science China Chemistry*, *64*, 877-878, https://doi.org/10.1007/s11426-021-9993-9

[17] S.A. Muhammed Ali, Ros Emilia Rosli, Andanastuti Muchtara, Abu Bakar Sulong, Mahendra Rao Somalu & Edy Herianto Majlan (2015) Effect of sintering temperature on surface morphology and electrical properties of samarium-doped ceria carbonate for solid oxide fuel cells, *Ceramics International*, *41(1-B)* 1323-1332, https://doi.org/10.1016/j.ceramint.2014.09.064

[18] Z.A. Qureshi, M.E.S. Ali, R.A. Shakoor, S. AlQaradawi & R. Kahraman (2024) Impact of synergistic interfacial modification on the electrochemical performance of LiNi0.5Mn1.5O4 cathode materials, *Ceramics International*, *50(10)*, 17818-17835, https://doi.org/10.1016/j.ceramint.2024.02.271

[19] S. Zare Ghorbaei & H. Ale Ebrahim (2020) Carbonation reaction of strontium oxide for thermochemical energy storage and CO_2 removal applications: Kinetic study and reactor performance prediction, *Applied Energy*, *277*, 115604, https://doi.org/10.1016/j.apenergy.2020.115604

[20] Aswathy M. Narayanan & Arun M. Umarji (2019) Optimization of absorption/desorption parameters of Brownmillerite $SrCoO_{2.5}$ for oxygen storage, *Journal of Alloys and Compounds*, *803*, 102-110, https://doi.org/10.1016/j.jallcom.2019.06.189

[21] Franklin & Marchall College (2019). *Materials characterization fundamentals*. Department of Education Open Textbook Pilot Project, the California Education Learning Lab. Retrieved Jun 8, 2025, from https://chem.libretexts.org/Courses/Franklin_and_Marshall_College/Introduction_to_Materials_Characterization__CHM_412_Collaborative_Text/Spectroscopy/Energy-Dispersive_X-ray_Spectroscopy_(EDS)#:~:text=Downloads-,Full,-PDF

[22] Fei Yang, Haixia Su, Yunqin Yang, Zhaodi Shen, Chun Zhang & Linwei Zhang (2025) A flexible porous electrospun carbon nanofiber cathode catalyst for rechargeable liquid and flexible Zn-air batteries, *Carbon*, *240*, 120372, https://doi.org/10.1016/j.carbon.2025.120372

[23] Swati Kumari, Sakshi Raturi, Saurabh Kulshrestha, Kartik Chauhan, Sunil Dhingra, Kovacs Andras, Kyaw Thu, Rohit Khargotra & Tej Singh (2023) A comprehensive review on various techniques used for synthesizing nanoparticles, *Journal of Materials Research and Technology*, *27*, 1739-1763, https://doi.org/10.1016/j.jmrt.2023.09.291

[24] Lun Feng, William G. Fahrenholtz, Gregory E. Hilmas, Jeremy Watts & Yue Zhou (2019) Densification, microstructure, and mechanical properties of ZrC–SiC ceramics, *Journal of the American Ceramic Society*, *102(10)*, 5786-5795, https://doi.org/10.1111/jace.16505

[25] Owen Jones-Salkey, Zoe Chu, Andrew Ingram & Christopher R. K. Windows-Yule (2023) Reviewing the impact of powder cohesion on continuous direct compression (CDC) performance, *Pharmaceutics*, *15(6)*, 1587, https://doi.org/10.3390/pharmaceutics15061587

[26] Umira A. Yusop, Hamimah A. Rahman & Kang H. Tan (2019) Effect of Ag Addition on the Structural properties of $Ba_{0.5}Sr_{0.5}Co_{0.8}Fe_{0.2}O_{3-\delta}$–$Sm_{0.2}Ce_{0.8}O_{1.9}$ composite cathode powder, *The International Journal of Integrated Engineering*, *11(7)*, pp. 169-175, https://doi.org/10.30880/ijie.2019.11.07.022

[27] Sicheng Jiang, Zhimin You & Ning Tang (2023) Effects of calcination temperature and calcination atmosphere on the performance of Co_3O_4 catalysts for the catalytic oxidation of toluene, *Processes*, *11(7)*, 2087, https://doi.org/10.3390/pr11072087

[28] Liu, G. Q., Hao, Q. B., Zheng, H. L., Zhang, S. N., Xu, X. Y., Jiao, G. F., Cui, L. J., Wang, P. F. & Li, C. S. (2018) Effect of grinding method on the precursor powder of Bi2223 and properties of strip, *Journal of Physics: Conference Series*, *1054(1)*, 012042, https://doi.org/10.1088/1742-6596/1054/1/012042

[29] Muhammed Ali Shaikh Abdul Kader Abdul Hameed, Andanastuti Muchtar, Jarot Raharjo & Deni Shidqi Khaerudini (2022) A Review on the process-structure-performance of lanthanum strontium cobalt ferrite oxide for solid oxide fuel cells cathodes, *International Journal of Integrated Engineering*, *14(2)*, 121-137, https://doi.org/10.30880/ijie.2022.14.02.017

[30] Heng, Li., & Mingwang, Fu. (2019) Deformation-based processing of materials: Behavior, performance, modeling, and control. Chapter 8 - Microstructure abnormality-related defects (pp. 277-319). Elsevier. https://doi.org/10.1016/C2017-0-01559-8

[31] Azreen Junaida Abd Aziz, Nurul Akidah Baharuddin, Mahendro Rao Somalu & Andanastuti Muchtar (2022) Layering Ooptimization of the $SrFe_{0.9}Ti_{0.1}O_{3-\delta}$-$Ce_{0.8}Sm_{0.2}O_{1.9}$ composite cathode. *Molecules*, *27(8)*, 2549, https://doi.org/10.3390/molecules27082549

[32] Ling Hu, Defeng Zhou, Xiaofei Zhu, Ning Wang, Jinghe Bai, Huifang Gong, Youjie Zhang, Yunlong Chen, Wenfu Yan & Qiurong Zhu (2024) A high-performance composite cathode based on thermal expansion complementation for SOFC, *Fuel*, *362*, 130864, https://doi.org/10.1016/j.fuel.2024.130864

[33] Nilam Shah, Tianjiu Zhu, Xiaoyong Xu, Hao Wang, Zhonghua Zhu & Lei Ge (2025) Synergistic thermal expansion reduction in cobalt-containing perovskite cathodes for solid oxide fuel cells, *Journal of Power Sources*, *654*, 237832, https://doi.org/10.1016/j.jpowsour.2025.237832

[34] Monika Singh & Akhilesh Kumar Singh (2019) Studies on structural , morphological , and electrical properties of Ga3+ and Cu2+ co-doped ceria ceramics as solid electrolyte for IT-SOFCs, *International Journal of Hydrogen Energy*, *45(44)*, 2-12, https://doi.org/10.1016/j.ijhydene.2019.09.084

[35] Mohammad Safi, Mohammad Kazem Hassanzadeh-aghdam & Mohammad Javad Mahmoodi (2019) Effects of nano-sized ceramic particles on the coef fi cients of thermal expansion of short SiC fiber-aluminum hybrid composites, *Journal of Alloys and Compounds*, *803*, 554–564, https://doi.org/10.1016/j.jallcom.2019.06.314

[36] Daniel Sikstrom & Venkataraman Thangadurai (2024) A tutorial review on solid oxide fuel cells: Fundamentals, materials, and applications. *Ionics*, 1-26, https://doi.org/10.1007/s11581-024-05824-7

[37] J. Madhuri Sailaja, N. Murali, K. Vijay Babu, & V. Veeraiah (2016) Effect of strontium on the phase structure of $Ba_{1-x}Sr_xCe_{0.65}Zr_{0.2}Y_{0.15}O_{3-\delta}$ ($0 \leq x \leq 0.25$) proton conductor by citrate–EDTA complexing sol–gel method, *Journal of Asian Ceramic Societies*, *5(1)*, 1–13, https://doi.org/10.1016/j.jascer.2016.12.004

[38] Alexandros Ch. Lazanas & Mamas I. Prodromidis (2023) Electrochemical Impedance Spectroscopy-A Tutorial, *CS Measurement Science Au*, *3(3)*,162-193, https://doi.org/10.1021/acsmeasuresciau.2c00070

[39] Sanaz Zarabi Golkhatmi, Muhammad Imran Asghar & Peter D. Lund (2022) A review on solid oxide fuel cell durability: Latest progress, mechanisms, and study tools, *Renewable and Sustainable Energy Reviews*, 161, 112339, https://doi.org/10.1016/j.rser.2022.112339

[40] Adi Subardi, Ade Indra, Jan Setiawan & Yen-Pei Fu (2023) Structural and electrochemical analysis of $SmBa_{0.8}Sr_{0.2}Co_2O_{5+\delta}$ cathode oxide for IT-SOFCs, *International Journal of Integrated Engineering*, *15(1)*, 173-179, https://doi.org/10.30880/ijie.2023.15.01.015

[41] Hui Deng, Wei Zhang, Xunyin Wang, Youquan Mi, Wenjin Dong, Wenyi Tan, Bin Zhu (2017) An ionic conductor $Ce_{0.8}Sm_{0.2}O_{2-\delta}$ (SDC) and semiconductor $Sm_{0.5}Sr_{0.5}CoO_3$ (SSC) composite for high performance electrolyte-free fuel cell, *International Journal of Hydrogen Energy*, *42 (34)*, 22228-22234, https://doi.org/10.1016/j.ijhydene.2017.03.089